On Modeling the RIS as a Resource: Multi-user Allocation and Efficiency-Proportional Pricing

Alexandros Papadopoulos, Dimitrios Tyrovolas, *Member, IEEE*, Antonios Lalas, Konstantinos Votis, Stefan Schmid, Sotiris Ioannidis, George K. Karagiannidis, *Fellow, IEEE* and Christos K. Liaskos

***Abstract*—Programmable Wireless Environments aim to render the communication environment a controllable, software-defined medium. Reconfigurable Intelligent Surfaces (RISes) are the key enabling technology, which can offer the real-time capability to manipulate impinging waves. RISes are expected to be widely deployed in B5G/6G networks to serve a large number of users simultaneously. Despite numerous analyses highlighting the benefits of utilizing previously unexploitable propagation factors through the use of RISes, there is a lack of analysis regarding their relation to the concept of network resource, their allocation to users/stakeholders and their fair pricing. Thus, this paper models RISes as networked resources. Based on this definition, the PRIME algorithm is proposed, the first algorithm for RIS resource allocation and joint pricing. PRIME strives for proportionality between the offered end-user performance level and the corresponding resource pricing, promoting fairness. The algorithm is evaluated through full-wave electromagnetic simulations, for various RIS functionalities and frequency bands.**

***Index Terms*—RIS, resource allocation, multiplexing, pricing.**

I. Introduction

The advent of new technologies towards Beyond-5G (B5G) and 6G wireless communications has fundamentally changed our perception of future communication paradigms. Until now, the propagation environment has been considered a given and uncontrollable factor, with phenomena such as fading and scattering being treated stochastically. However, in new wireless technologies, the environment is viewed as a set of programmable resources that can be optimally configured, transforming the entire system setting into a Programmable Wireless Environments (PWE) [1].

The main technology driving this transformation are the Reconfigurable Intelligent Surfaces (RISes). An RIS can interact with impinging electromagnetic (EM) waves in real-time and in a software-defined manner [2]. This interaction aims to effectively utilize previously uncontrollable resources, such as the scattering behavior of passive objects, significantly improving the Quality of Service (QoS) for users.

At the system level, PWEs are created by coating all planar surfaces within an area with RISes. Each separate RIS can then be programmed in terms of its interaction with impinging waves, e.g., creating cascading paths and reaching non-line-of-sight areas (nLos). In this context, the EM propagation within a space can be dynamically manipulated, benefiting the users in real-time [1].

As noted, he most characteristic feature of PWEs is their capability to reconstruct LoS channels between base stations and users. However, this is not the most challenging feature of PWEs. Signals can also be kept away from specific areas, creating "quiet zones" within the network and enhancing its physical security [3]. Additionally, PWEs can enhance safety through improved object detection and localization features [4]. Lastly, the significant impact of the Doppler effect [5], especially in V2X communication links, can be mitigated by ensuring the direction of arrival of signal remains perpendicular to the trajectory of a mobile user.

Within the PWE, as with almost any other components in a communication network, each RIS unit will need to simultaneously serve multiple users with different requirements. In networking terms, each RIS is a resource that should be shareable among users. The definition of the RIS-as-a-resource, and its efficient allocation across multiple users should be clearly described, in orded to be integrated to the policy of the stakeholder managing the infrastructure containing the PWE.

The transformation of well-established resource allocation strategies in already existing technologies [6] can boost the same procedures in the context of PWEs. One such strategy is the division of a RIS unit into multiple virtual ones [7]. Beyond existing knowledge, dedicated frameworks for serving multiple users with RIS have already been proposed and discussed [8]. Nonetheless, a gap exists in the precise manner in which the RIS resource will be defined and be allocated to network users in accordance with their pricing levels, in accordance with their service-level agreements.

In this context, our research contributions are as follows:

- We define the notion of RIS as a networked system resource.
- Subsequently, we present the first resource allocation algorithm, aligned to our resource definition. The algorithm supports multiple RIS functionality types and can be adapted to any pricing policy. A fair pricing policy is provided as a default.

A. Papadopoulos is with the Computer Science Engineering Department, University of Ioannina, Ioannina, Greece and with the Information Technologies Institute, CERTH, Greece (e-mail: a.papadopoulos@uoi.gr/alexpap@iti.gr).

D. Tyrovolas is with Aristotle University of Thessaloniki, Greece (email: tyrovolas@auth.gr).

A. Lalas and K. Votis are with the Information Technologies Institute, CERTH, Greece (e-mails:{lalas, kvotis}@iti.gr

S. Schmid is with TU Berlin and Fraunhofer SIT, Berlin, Germany (email: stefan.schmid@tu-berlin.de).

S. Ioannidis, Technical University of Chania, Greece (sotiris@ece.tuc.gr).

G. K. Karagiannidis, Aristotle University of Thessaloniki, Greece; Cyber Security Systems and Applied AI Research Center, Lebanese American University, Lebanon (geokarag@auth.gr).

C. K. Liaskos is with the Computer Science Engineering Department, University of Ioannina, Ioannina and with the Foundation for Research and Technology Hellas (FORTH), Greece (e-mail:cliaskos@uoi.gr).

- We evaluate the algorithm's efficiency via realistic, full-wave EM simulations. Moreover, we deduce the computational complexity of the algorithm, noting its applicability to real-world scenarios.

The rest of this paper is organized as follows: Section II provides the prerequisite knowledge. Section III presents the related studies. Section IV defines the notion of RIS as a networked resource, while Section V elaborates on the resource allocation algorithm proposed in this paper. The evaluation of the algorithm is presented in Section VI. Section VII discusses potential research challenges, and Section VIII offers conclusions.

II. Prerequisites

The RIS technology is based on the principles of metamaterials, which are artificially engineered structures created by connecting basic units known as unit cells. From a macroscopic perspective, a RIS appears as a thin, planar, and rectangular device, resembling a tile, composed of an array of these unit cells. Within these tiles, various active elements [9], such as PIN diodes [10] or MEMS [11], [12], are embedded. Controlling these active elements enables the RIS to manipulate impinging EM waves propagation across its surface in a software-defined manner.

Specifically, when an EM wave impinges on the RIS surface, it induces a specific current distribution. This distribution is strongly connected with the state of all of its active elements, which is referred to as the RIS *configuration*. By properly determining the RIS configuration, the incident EM wave can be effectively manipulated, leading to various macroscopic responses, known as RIS *functionalities*. These include beam steering, beam splitting, perfect absorption, modulation of the wavefront's phase, amplitude, and/or polarization, as well as wavefront sensing [13].

Defining the optimal RIS configuration for a specific functionality is a complex and time-consuming optimization task [14]. Therefore, it is not usually feasible to compute this during the RIS operation phase. Instead, this task is completed during the manufacturing phase. During this phase, the functionalities supported by the RIS unit are matched with the optimal RIS configuration by combining knowledge gained from physics insights and metaheuristic tools, within a simulation tool or prototyped measurement system [14]. These mappings are saved in a Codebook Database. Consequently, once the RIS is in the operation phase and needs to achieve a specific functionality, it only needs to retrieve the corresponding entry from the codebook [1].

The RIS technology is towards its integration into current communication networks. Thus, it will soon need robust mechanisms to serve multiple users simultaneously. The most efficient and straightforward way to make real-time serving of multiple users feasible is through the multiplexing of codebook entries [15]. This means that multiple users share the RIS elements, whose values are determined based on all the respective codebook entries.

An algorithm that can efficiently multiplex the codebook entries is COMMON [15], [16]. The COMMON algorithm retrieves the codebook entries for the users from the respective database, pre-processes them, and then sets each RIS element to the most frequent value among the codebook entries resulting to the final, common RIS configuration. Its workflow is presented in Alg. 1.

Algorithm 1: Codebook Multiplexing Algorithm (COMMON)

Input: Dimensions of RIS (M, N), Number of users K, discretization parameter N_d, Codebook Entries CE_k
Output: Common RIS configuration $CC(M, N)$
Initialization: Discrete Entries DE_k
Discretization function $f_{dis}(N_d)$*:*
for $k = 1$ to K **do**
  $DE_k \leftarrow f_{dis}(CE_k, N_d)$
end for
Initialize $CC(M, N)$ to store the final RIS configuration
for each element (m, n) in CC **do**
  Initialize an empty list $values$
  for $k = 1$ to K **do**
    Append $DE_k(m, n)$ to $values$
  end for
  Determine each element value with the most frequent one
  $CC(m, n) \leftarrow$ ComputeMostFrequent$(values)$
end for
return CC

The RIS resource allocation procedure, in addition to the definition of the common RIS configuration, also requires a pricing mechanism to ensure that the sharing of RIS elements leads to the proper distribution of the resources to each user. Since COMMON lacks such a mechanism, in this paper, we introduce the PRIME algorithm (Sec. V).

III. Related Work

The research bibliography includes numerous proposals for the dynamic allocation of resources in various networks types. The primary challenge faced by the proposed algorithms, known as schedulers, is balancing the task of ensuring the satisfaction of a dynamically changing number of users' performance with the imperative of minimizing the allocation decision time [6]. Additionally, within the same network, there may be diverse user groups with different pricing offers. These pricing differences should be considered in the performance results to ensure fairness [17].

Moreover, many studies collectively advance the field of network slicing and resource allocation, presenting diverse methodologies to enhance network performance and efficiency. For instance, addressing congestion and route efficiency, [18] employs an optimization method to minimize congestion and route lengths with fewer links between transmitters and receivers. In mobile edge computing systems, [19] investigates network slicing using a combination of heuristic tools and Lyapunov optimization techniques to maximize the operator's revenue both in the short and long term.

figures/algorithm_description.png

Fig. 1: The resource allocation procedure in a RIS-assisted environment with the integration of PRIME algorithm.

Additionally, [20] presents a radio access network (RAN) slicing method that flexibly allocates RAN resources using deep reinforcement learning. The challenge of fairly sharing multiple resources when network resources are insufficient is addressed in [21], which proposes an optimization framework using the Ordered Weighted Average operator. Lastly, the study [22] proposes a machine learning-based RAN slicing allocation strategy, incorporating LSTM models to maximize spectrum efficiency and maintain service satisfaction ratios despite user mobility.

Another well-established tool for resource allocation is virtual switching. It has emerged as a pivotal technique for resource allocation and network slicing, where the core network is virtualized to serve different users. This is demonstrated in [23], which implements virtual networking in data centers and cloud computing infrastructures. Similarly, in [24], the authors introduce an iterative optimization framework for resource allocation among the network owner, the cloud owner, and the slice network owner to ensure optimal bandwidth distribution. Finally, in [25], the Virtual Network Embedding Problem is analyzed, utilizing randomized rounding of Linear Programming solutions for resource allocation. Building on this approach, [7] introduces the concept of a Virtual Programmable Metasurface (VPM), an idea closely aligned with the widely known Virtual Machine concept. VPMs are designed as software entities that encapsulate a specific subset of the RIS physical elements, simplifying their management and control.

Concerning specifically the optimization of RIS-assisted networks, several proposals have been made. In [26], reinforcement learning is used to optimize the transmit power of base stations and the state of RIS elements. This issue is also discussed in [27], where a supervised solution is proposed. In [28], the maximization of the network's energy efficiency is addressed using the SCA method. Lastly, in [29], federated learning is employed to minimize the system's power expenditure.

The common goal of the mentioned papers is to optimize the network's parameters, thereby obtaining significant performance gains for the users. However, the method of allocating these resources to the network's users is a different challenge, and the suggested frameworks for this task are notably limited.

In [8], a resource-sharing model for PWE is introduced. The primary concept involves the concurrent provision of multiple functionalities through the segmentation of each RIS. Each RIS tile or group of tiles is assigned to specific tasks. The proposed algorithm then allocates competing user requests based on weighted policies, ensuring a Time-Division-Multiple-Access (TDMA) style of resource sharing in the PWE. Similarly, in [30], RIS multi-tasking involves the use of time duty-cycling, where each user is allocated specific time slots during which they are served by a RIS unit.

It is essential to consider that the RIS unit manages the desired manipulation of EM waves due to its total area. Splitting the RIS into multiple segments may lead to lower performance for all users. As for TDMA, this method requires stringent synchronization. Additionally, latency due to the alignment of the elements' values at the hardware level with the desired values in each time-frame must be considered. Furthermore, due to the nature of TDMA, when a specific user is served by the RIS unit, no gains are achieved for the remaining users.

In contrast, in our previous work [15], we proposed the COMMON algorithm, which is presented here as Alg.1. This algorithm efficiently multiplexes the RIS configurations of each user into a common one, thereby enabling the concurrent serving of multiple users.

PRIME is the first algorithm dedicated to allocating RIS resources to multiple users with different pricing levels. As depicted in Fig.1, PRIME is integrated into the Telecommunication Stakeholder Operation Center. Users participate in the network based on the defined pricing policy, and the supported RIS functionalities are available as codebook entries in the dedicated database. PRIME's objective is to effectively combine these two components.

The PRIME algorithm determines the common RIS configuration by allocating its elements according to each user's pricing policy. This configuration is then sent to the RIS controller to ensure proper alignment of the microscopic RIS state. Users with higher pricing levels have a greater influence on the RIS configuration, ensuring a proportional relationship between user performance and pricing level.

IV. Definition of RIS as Network Resource

In order to define the notion of the RIS resource, we employ the notion of EM functions [31]. As noted, these are macroscopic descriptors of the manipulation exerted by the RIS to the impinging wave. They are expressed in software terms, i.e., as functions with well-defined input and output data.

For instance, the $\texttt{PLANAR\_ABSORB}(\overrightarrow{r}) \rightarrow \emptyset$ function describes the full absorption of a planar wave impinging on the RIS from a direction $\overrightarrow{r}$. The $\texttt{PLANAR\_STEER}(\overrightarrow{r}) \rightarrow \overrightarrow{d}$ describes the reflection or refraction of a wave impinging from direction $\overrightarrow{r}$ to direction $\overrightarrow{d}$. The $\texttt{PLANAR\_SPLIT}(\overrightarrow{r}) \rightarrow \left[\left\{\overrightarrow{d_1}, p_1\right\}, \ldots\right]$ described the reflection or refraction of the impinging wave into a set of different directions, $\overrightarrow{d}_i$, each carrying a portion, p_i, of the power of the original, impinging wave. Notice that function, f, must have a corresponding set of RIS element states, σ_{ij}, such that $\sigma_{ij} \rightarrow f$. In other words, setting the RIS elements to the states σ_{ij} yields the macroscopic function f. The definition of σ_{ij} depends on the RIS design and can be, e.g., cell phases, cell impedances, or even voltages applied to embedded actuators.

The above EM function examples are ideal in terms of performance. In practice, each has a degree of efficiency, ϵ, when implemented, e.g., due to material losses, RIS design specifications or RIS multitasking (i.e., serving two or more EM functions at the same time). Extending the notation, we can exemplary write $\texttt{PLANAR\_ABSORB}(\overrightarrow{r}) \rightarrow \epsilon$, and $\epsilon : \texttt{PLANAR\_STEER}(\overrightarrow{r}) \rightarrow \overrightarrow{d}$. The definition of ϵ can be adapted depending on the set system specifications. E.g., for $\texttt{PLANAR\_ABSORB}(\overrightarrow{r})$, it can be defined as either the maximum reflected or refracted power towards any direction, or as the attenuation degree of the impinging wave. For $\texttt{PLANAR\_STEER}$ it can be defined as the gain towards the intended direction of departure, the ratio of power towards $\overrightarrow{d}$ divided by the total reradiated power, etc.

Complimenting the requirements for defining the RIS resource notion, note that a RIS has been shown to be able to serve many EM functions simultaneously [15]. In particular, for a set of functions $\epsilon_1 : f_1 \rightarrow \sigma_{ij}^{(1)}$, ..., $\epsilon_k : f_k \rightarrow \sigma_{ij}^{(k)}$, ..., $\epsilon_n : f_n \rightarrow \sigma_{ij}^{(n)}$, there exists a single $\sigma_{ij} : \sigma_{ij}\left(\sigma_{ij}^{(1)}, \ldots, \sigma_{ij}^{(k)}, \ldots \sigma_{ij}^{(n)}\right)$ such that:

$$\sigma_{ij} \rightarrow \{\epsilon_1' : f_1, \ldots, \epsilon_k' : f_k, \ldots, \epsilon_n' : f_n\}. \tag{1}$$

Notice that the merging of $\sigma_{ij}^{(1)}, \ldots, \sigma_{ij}^{(k)}, \ldots \sigma_{ij}^{(n)}$ into σ_{ij} yields the same functions, but alters the efficiency of each.

With the above definitions, we proceed to define the notion of the RIS resource, by first drawing a parallelism to a more common and well-understood resource, the CPU. A CPU is a resource shared by applications. When a single application is running on a CPU, it is allotted the full number of clock ticks per second that the specific CPU can offer. When a number of additional applications is running on the same CPU, the original application gets a reduced number of clock ticks.

The resource slice is the ratio of the new allotted clock ticks, divided by the full number of clock ticks allotted when ran alone on the CPU.

Based on the above, we define the following:

Definition 1. A RIS is a resource that is shared by macroscopic EM functions.

Moreover:

Definition 2. The resource slice allotted to an EM function, f, is defined as the ratio r such that

$$r_f = \frac{\epsilon'}{\epsilon} \tag{2}$$

where ϵ is the efficiency of f when hosted alone on the RIS, and ϵ' is its efficiency when hosted with other EM functions on the same RIS, $\sigma_{ij} \to \{\epsilon' : f, \ldots, \epsilon'_k : f_k, \ldots, \epsilon'_n : f_n\}$.

V. PRIME: A Novel Algorithm Scheme for Sharing & Pricing

In this section, we present the PRIcing-based Multiplexing of codebook Entries (PRIME) algorithm. PRIME, mainly, is dedicated to the definition of r_f factor of Eq. 2 and its workflow is presented in Alg. 2. It is designed for allocation of the RIS resources via the pricing-based multiplexing of codebook entries. PRIME ensures that each user's performance reflects their pricing level.

The required inputs for the algorithm include the dimensions of the RIS (M, N), the total number of users K utilizing the RIS unit for enhanced performance within the communication network, and a discretization parameter N_d. Additionally, the algorithm must have access to the Codebook Database, which contains the entries for the optimal RIS configuration for each user. It is important to note that the computation of these codebook entries is not part of the algorithm and is assumed to be an input.

The adaptation of the PRIME to the existing pricing levels of the stakeholders' police is established via the definition of the Payment Factor (PF). The PF is an integer and positive value assigned to each user once they enter the resource allocation procedure. Each stakeholder can define as many discrete values for PFs as they want and assign values that reflect quantitatively the differences in the performance received by users with various pricing levels. The PFs of all the users have to be given to the algorithm also as input.

PRIME begins by retrieving the codebook entries, CE, matching the user requests for a RIS functionality. Next, it discretizes all the elements of CE based on the discretization parameter N_d leading to the DE matrices. Using the PF values, the algorithm then creates an equal number of replicas for each DE_k, which is why PFs must be natural numbers. After generating all the replicas of the discretized values, the algorithm determines the common RIS configuration, CC, by selecting the most frequent values among the replicas for each RIS element. As is evident, users with higher PF values have a greater influence on the CC due to the increased number of replicas of their entries that participate in the final selection, ensuring the pricing part of the PRIME.

Algorithm 2: PRIcing-based Multiplexing of codebook Entries (PRIME)

Input: Dimensions of RIS (M, N), Number of users K, discretization parameter N_d, Codebook Entries CE_k, Payment Factors PF_k
Output: Common RIS configuration $CC(M, N)$
Initialization: Discretize CE_k to DE_k
Discretization function $f_{dis}(N_d)$*:*

```
for k = 1 to K do
    DE_k ← f_dis(CE_k, N_d)
end for
Replica Creation based on Payment Factors:
Initialize an empty list replicas
for k = 1 to K do
    Append DE_k to PF_k replicas
end for
Initialize CC(M, N) to store the final RIS configuration
Determine each element value with the most frequent one
for each element (m, n) in CC do
    CC(m, n) ← ComputeMostFrequent(replicas)
end for
return CC
```

The evaluation of the algorithm's feasibility in real-world applications is closely tied to the computational time required for pricing-based codebook entries multiplexing. Analyzing the algorithm's workflow, the computational complexity depends on PF values, the dimensions of the RIS unit, and the total number of users.

First, the algorithm discretizes the codebook entries for each user across the RIS elements, resulting in a computational complexity of $O(KMN)$. Next, the algorithm generates configuration replicas based on each user's PF values, adding another layer of complexity. These replicas are then combined, resulting in a computational complexity proportional to the number of users and their respective PFs. Consequently, this part of the algorithm incurs a complexity equivalent to the sum of all PF values, denoted as $O(\sum PF)$. Therefore, the overall computational complexity of the PRIME algorithm is expressed as $O(KMN + \sum PF)$.

VI. Evaluation

In this section, the PRIME algorithm is evaluated using full-wave EM simulations. We investigate the critical relationship between each user's received performance and their respective PF. A novel efficiency metric is defined, allowing for the comparison of PRIME with alternative approaches. Finally, we discuss the computational time required for PRIME on different hardware setups.

A. PRIME application based on full-wave EM simulations

First, we assess the capability of the PRIME algorithm to efficiently allocate the RIS elements according to each user's pricing level, as expressed by the PF. The evaluation is conducted using full-wave EM simulations. In the following, we present the evaluation setup, the application of PRIME algorithm and a discussion of the main conclusions.

1) System Model: The communication network consists of 4 different base stations. The total number of users are 5 and there is one RIS unit. To encompass a more general concept, two users are served by the same base station, while the remaining three are served by different ones.

2) Scenario: The LoS connection between the users and their respective base stations is blocked. The users are positioned opposite a RIS unit with the goal of restoring the LoS connection. The RIS unit elements are shared among the five users. The resource allocation is established via a PF assigned to each user. Each user's PF is unique.

3) Physical layer: The RIS unit used during the full-wave EM simulations has been introduced in our previous work [14]. In this design, depicted in Fig. 2, the RIS unit cells consist of gaps between square metal patches, bridged by lumped complex impedance loads. These patches are positioned on a metal-backed dielectric substrate and a thin metal sheet that serves as a ground plane. Specifically, the substrate is Rogers RT/Duroid 5880, which has an electric permittivity, ε_r, of 2.2, a tangent loss, $\tan\delta$, of 0.0009, and a thickness of 1.016 mm. The ground plane, like the square patches, is a perfect conductor with a thickness of 17.5 µm. There are 6 square patches on the y-axis and 12 on the x-axis. The number of tunable loads is 66. This cell design eliminates transmission and offers wide angular and spectral bandwidth. The value of its embedded load allows control over the amplitude and phase of the reflected wave in the x polarization.

4) Metrics of Performance: The EM energy flow between the base station (BS) and the user (UE) is estimated using the S21 parameter [32]. The S21 parameter, also known as the transmission coefficient, measures the signal transmission from port 1 to port 2 in a network. In our case, we compute the S21 parameter between each user and their respective base station. When the transmission coefficient is very low, it indicates that the LoS between the BS and the UE is blocked. The goal of positioning the RIS is to provide the $BS \rightarrow$ RIS $\rightarrow UE$ path to maximize the transmission coefficient for each user.

5) Tools & Creation of The Codebook Database: The full-wave EM simulations that are utilized for the evaluation of the PRIME algorithm have been conducted via measurements in an open solver called openEMS [33]. (For the remainder, "measurements" refer to full-wave EM simulation results.)

As mentioned previously, only the pricing-based multiplexing, not the computation of the codebook entries, is part of the PRIME algorithm. Therefore, the optimal RIS configuration for each user when served individually by the RIS must be measured and saved in the Codebook Dataset. For this procedure, we use the Physics Informed Codebook Compilation Software (PICCS) introduced in [14]. PICCS combines physics insights with metaheuristic tools. In our case, the optimization for computing the codebook entries is based on the NSGA-II algorithm [34]. This procedure generates a codebook entry for each user, consisting of 66 values for

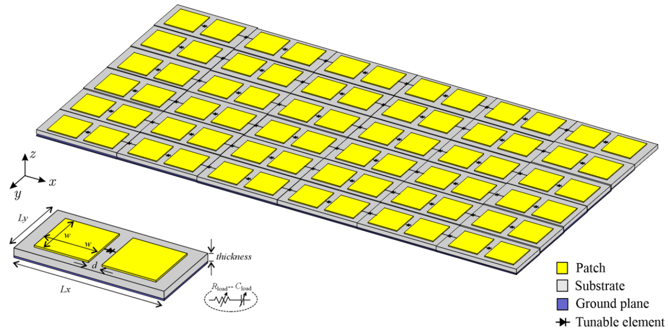

Fig. 2: The design of the RIS unit used in EM measurements for PRIME evaluation.

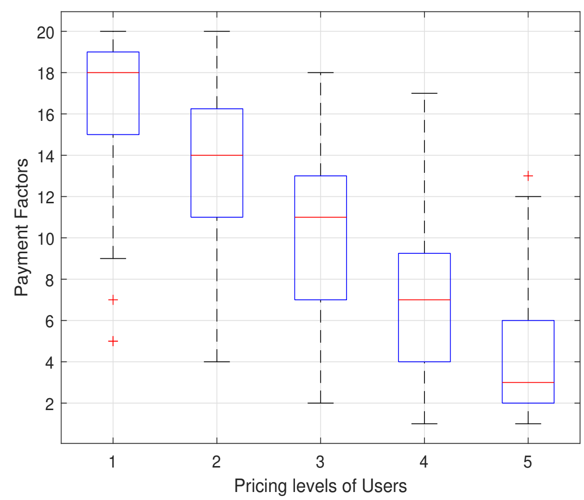

Fig. 3: Boxplot of the PF per pricing level of the combinations.

impedance capacitance. The impedance values range from 0.4 to 0.9 µF.

6) PRIME operation: The PRIME algorithm retrieves the codebook entries from the Codebook Database and multiplexes them according to the PFs assigned to each user. For the sake of generality of the evaluation, 205 combinations of PFs are assigned to the users. (For the remainder, the term combination will refer to the set of PF values that are assigned to the users each time.) The assignment of the PFs is a random procedure. The values vary from 1 to 20. The PRIME uses a discretization parameter of 0.05 for the determination of the common RIS configuration, CC.

In Fig. 3, the values of the PF combinations are depicted. Users with higher PF values have an average PF of 16.8 with a standard deviation of 3.07, whereas users with lower PF values have an average PF of 4.8 with a deviation of 2.82. Within each combination, since no user shares the same PF value with another, five distinct pricing levels are formed.

The measurements of S21 for each user, once the RIS is set with CC, are computed for each combination of PFs. Since the use of PICCS ensures that the codebook entries include the optimal RIS configuration for serving each user individually,

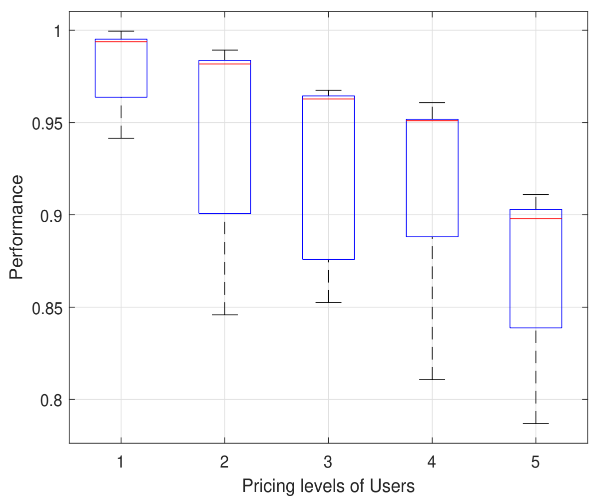

Fig. 4: Boxplot of the users' performance per pricing level with PRIME.

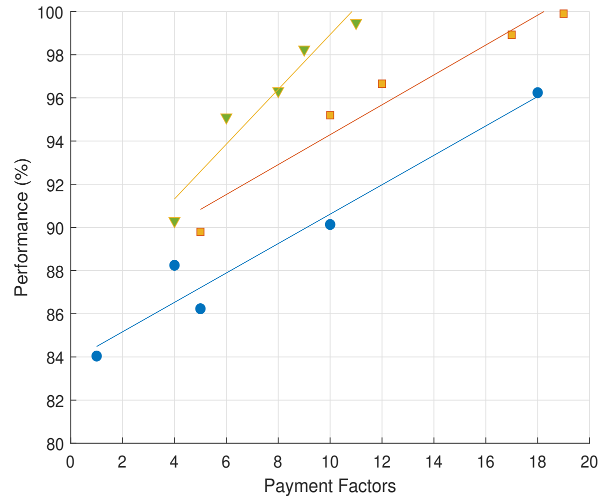

Fig. 5: The linear relationship between users' PF and performance with the usage of PRIME.

the performance for the allocation of RIS resources with respect to user k during combination c is calculated as follows:

$$P_{kc} = \frac{S21_{opt_k} - S21_{kc}}{S21_{opt_k}} \tag{3}$$

The performance values for each user during the different combinations are depicted in Fig. 4. The average values for users, from highest to lowest, are 98%, 94%, 93%, and 87%, with variations of 2%, 5%, 4%, 3%, and 2%, respectively. As is evident, the measurements confirm that the PRIME can effectively allocate the RIS resources via the proper sharing of its elements for multiple users with different pricing levels.

B. Relationship between PF and the users' performance levels

An aspect that requires further assessment is the relationship between each user's PF and their performance. PRIME offers a linear relationship between the assigned to each user PF and the received performance [16]. This relationship is verified in Fig.5, where three random combinations and their respective PFs and performance values are illustrated.

The intercept of this line primarily represents the minimum efficiency level, indicating the performance that a basic user receives. The slope of the line denotes the performance enhancement achieved with the addition of each PF unit, as defined by telecommunication stakeholders. Accurate estimation of the intercept and slope in each network, combined with the PF assigned to each user, allows for easy approximation of their performance.

he intercept and the slope of PRIME's performance line are strongly influenced by the total number of users [16]. As a next step, we also investigate how the intercept and the slope are affected by the users' PF. This analysis aims to determine how the performance of a specific user with a given pricing level can be affected by the other users participating in the same network. To this end, we perform a correlation analysis between the PF assigned to all users and the performance received by an individual user.

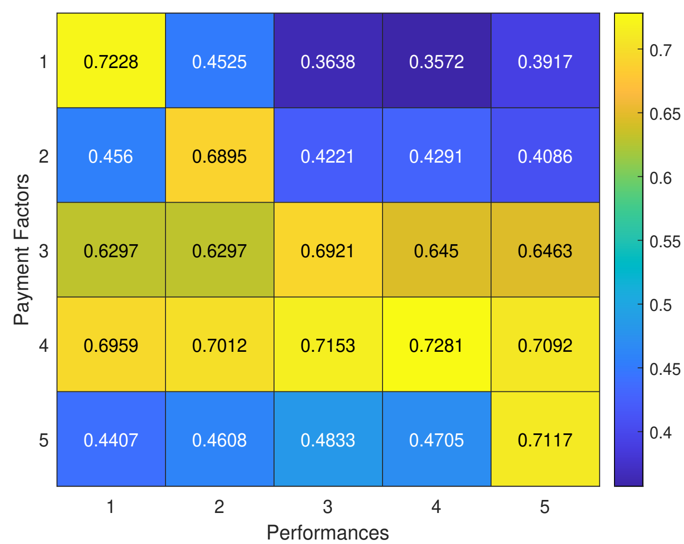

Fig. 6: The correlation matrix among all users' performance and PF values.

The correlation measures the strength and direction of the relationship between two variables, ranging from -1 (perfect negative correlation) to 1 (perfect positive correlation), with 0 indicating no correlation. As mentioned previously, no users have the same PF value in any combination. Therefore, we can shape five different pricing levels. Subsequently, we investigate the correlation between each PF value and the corresponding performance. The results are illustrated in Fig. 6.

The highest correlation is observed between each user group's PF values and their respective performance (major diagonal elements in Fig. 6). However, there is also a significant correlation with other PF user groups, ranging from 0.3572 to 0.7153. The highest correlations are seen in the groups with mid-level PF values, with a notable correlation greater than 0.6297, indicating a relatively strong relationship.

Having detected the correlation between user groups and

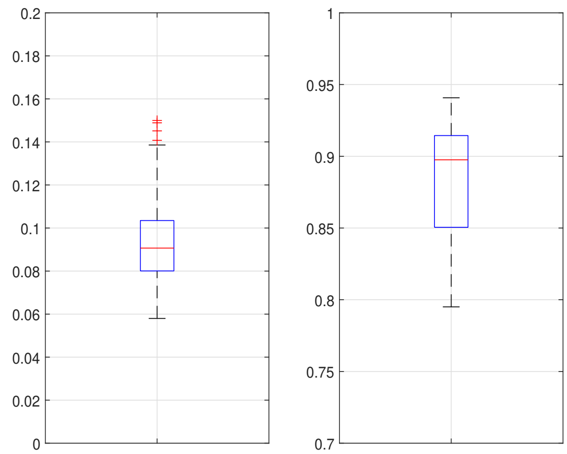

Fig. 7: Boxplot of the slope (left) and the intercept (right) of the performance line based on the PFs of the pricing levels.

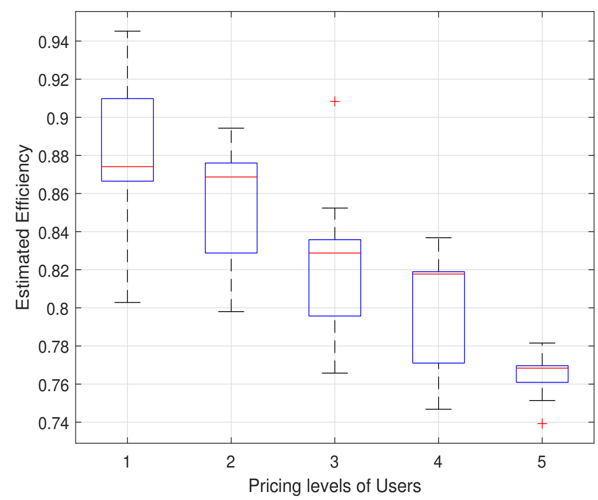

Fig. 8: Estimation of the RIS resource allocation achieved by PRIME

performances, the objective analysis for intercept and slope of the performance line follows. For this task, we scale the PF values during each combination. Therefore, each scaled PF value is mapped in relation to the PF values of the rest users. After this action, each scaled PF is aligned with the respective performance, and the intercept and the slope factors are computed. The respective boxplot is illustrated in Fig. 7.

The mean value of the slope is 0.0928, with a standard deviation of 0.0185. For the intercept, the mean value is 0.8820, with a standard deviation of approximately 0.04. This indicates that PRIME ensures that all users can achieve performance levels between 84% and 92%, while users with higher PF values can approach 100% performance. A higher PF ensures that, irrespective of the PF values of the other users and the total number of them, the performance will be close to optimal.

C. Evaluation via a novel RIS resource allocation efficiency metric

In this section, we present a proposal for a metric to estimate the allocation efficiency for each user during the RIS resource sharing. This metric is based on the deviation between the configuration of the RIS elements when the user is served alone (codebook entry, CE) and the common RIS configuration (CC), as calculated in 4.

$$D_k(i,j) = CE_k(i,j) - CC(i,j) \tag{4}$$

It has been shown that the deviation in each RIS element does not have the same effect on its macroscopic response. For this reason, the metric also incorporates this physical aspect by computing the contribution of each deviation using 5.

$$AD_k(i,j) = D_k(i,j) \times Con(i,j) \tag{5}$$

The final efficiency per user is computed by subtracting 1 (the optimal case) from the sum of the resulting products of Eq. 5, as:

$$eff_k = 1 - Loss_k = 1 - \sum_{i,j} AD_k(i,j) \tag{6}$$

Having computed the accurate performance for each user, we use these measurements to evaluate the accuracy of the proposed metric. Using the same combinations for PF values, we also calculate the efficiency using this metric. The results are presented in Fig. 8.

The average efficiency, from higher to lower PF, is 88%, 86%, 82%, 80%, and 77%, with deviations of 5%, 4%, 3%, 3%, and 3%, respectively. Comparing Fig. 4 and Fig. 8, it is evident that the proposed metric has values approximately 8-11% lower than the actual performance values. This indicates that the proposed metric is a strict and reliable estimator for assessing the efficiency of any allocation method for RIS resources among multiple users with different pricing levels.

D. Comparison of PRIME and COMMON

COMMON can multiplex codebook entries so that the same RIS unit can simultaneously serve multiple users. PRIME can accomplish the same task, but with the added capability of considering unique pricing levels for each user and assigning priorities accordingly. Essentially, COMMON can be viewed as a special case of PRIME where all users share the same pricing level.

To compare COMMON and LEVEL, we use the efficiency estimator from Sec. VI-C. We assume that a 100x100 RIS unit is serving 10 users simultaneously, with a discretization parameter of 0.05. As shown in Fig. 9, PRIME assigns PFs to each user incrementally, starting from 1 and increasing to 10 (with User ID=1 assigned PF=1, User ID=2 assigned PF=2, and so on).

Fig. 9 demonstrates that COMMON can effectively share the RIS by multiplexing codebook entries, resulting in an efficiency of approximately 57% for all 10 users. Regarding the PRIME algorithm and the associated sharing and pricing

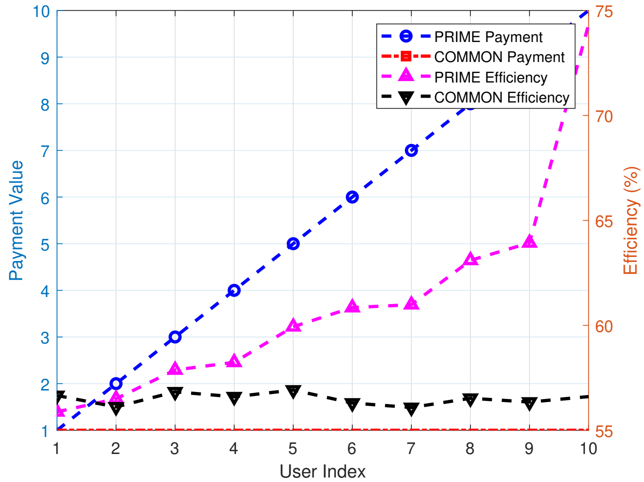

Fig. 9: User efficiency for PRIME and COMMON algorithms

results, it is clear that the improved efficiency levels of high-PF users do not come at the expense of others, ensuring network fairness. The higher PF values can achieve efficiencies about 27% higher.

E. Required computational time with different hardware setups

We also evaluate PRIME's required time using different hardware setups. Specifically, the first setup involves only a CPU, while the second setup utilizes both a CPU and a GPU. In both scenarios, the RIS dimensions are set to $M = N = 100$. The total number of users ranges from 5 to 50, and the PF values vary from 5 to 100. The codebook entries are multiplexed using MATLAB.

In the scenario where only the CPU is used, if the maximum PF value is below 70 for all user counts, the computational time remains under 100 ms (Fig. 13a). For higher PF maximum thresholds, the computational time increases to approximately three times that, reaching about 350 ms. Conversely, employing a GPU unit leads to a reduction in these values by up to 6 times (Fig. 13b). Specifically, when the PF maximum value does not exceed 70, the computational time is within the range of 10-20 ms. Even in more demanding cases, such as when there are 50 users and the PF maximum value is 100, the required computational time is around 60 ms.

Furthermore, it is acknowledged that MATLAB is recognized for its relatively slower performance compared to other programming languages like C/C++ or Fortran. This underscores the practicality of the proposed algorithm in determining RIS configurations to efficiently serve multiple users with high PF values in realistic scenarios, particularly in terms of computational demands.

F. Resource allocation in RIS-cascaded links

In a RIS-assisted environment, multiple RIS units will be placed in order to serve simultaneously many users. Firstly, we consider that 5 users are served from 2 RIS units that are

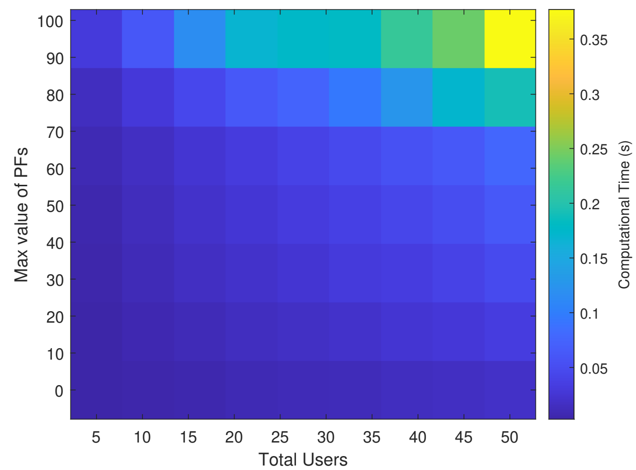

(a) CPU usage only.

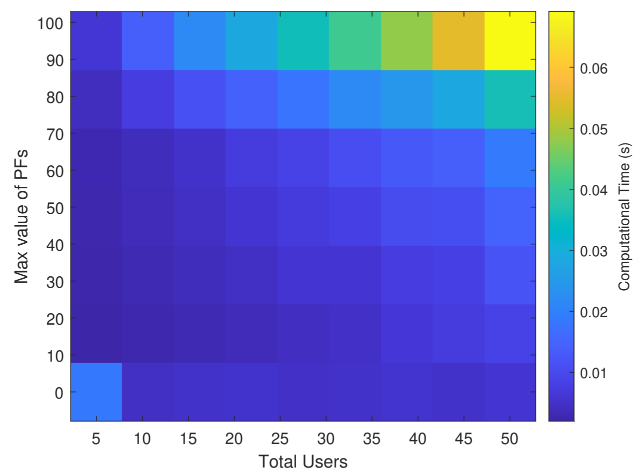

(b) GPU-driven calculations.

Fig. 10: Heatmaps of the PRIME's required computational time with respect to the total number of users and the maximum PF value.

50×50. For each user-RIS pair, the CE has been computed during the manufacturing phase. The user could be served by the same or different base station. Moroevoer, the operation frequency remains agnostic. The only essential for PRIME information is the CE. The PFs vary from 1 to 10.

In the Fig. 11, the efficiency of each user is illustrated as the average of the efficiency of each RIS unit as it has been defined in Sec. VI-C. As it is clear the PRIME can also allocate efficiently in this cascaded scenario.

However, the even more interesting and realistic scenario is the existance of multiple users with multiple RIS that try to be served in a communication link where any user is served by specific RIS and not from all of them. A such example is described in

VII. Open Challenges

In this paper, we presented PRIME, the first algorithm dedicated to RIS resource allocation for users with different pricing

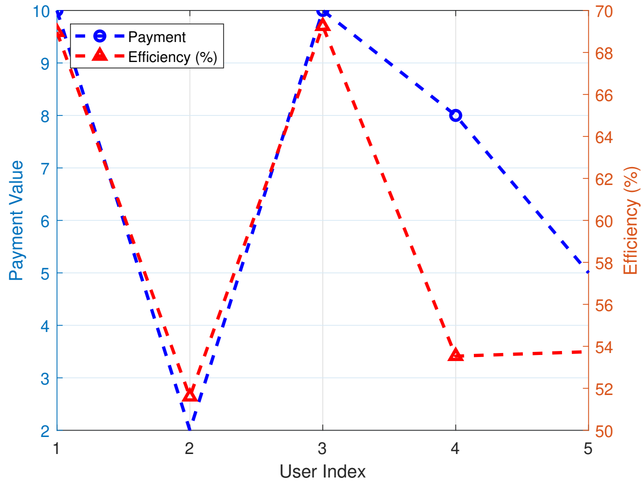

Fig. 11: The average efficiency of 5 users with 2 RIS units

levels, based on the multiplexing of codebook entries. The development of more algorithms aligned with the definition of the RIS-NET should continue, with these algorithms being evaluated against each other to establish the optimal solution in terms of performance and computational complexity.

These algorithms should focus on controlling the acceptable deviation between the individual codebook entries and the common RIS configuration. Furthermore, the cooperation of existing powerful metaheuristic tools should also be examined. Another topic to explore is the case of a full PWE, where multiple RIS units participate in the resource allocation of multi-hop communication links. In all these activities, the estimator proposed and evaluated in this paper could be utilized for accurate and fast computations.

An additional open challenge is leveraging the sharing ability of these algorithms to achieve more complex RIS functionalities. An indicative example of such functionality is beam splitting. In current approaches, beam splitting is treated as a complex optimization problem that tries to define the RIS configuration based on multiple users' positions. Instead, it could be addressed as a simple, pricing-based or not, multiplexing of various beam steering cases.

VIII. Conclusion

In this paper, we defined the notion of RIS as a share-able resource. This definition involves a mathematical procedure that aligns the sharing method of RIS elements to minimize the performance loss between the single-user scenario and the multi-user case. In this procedure, the pricing level of each user is used to assign a proportional weight.

Moreover, we propose and present PRIME, the first algorithm dedicated to pricing-based RIS resource allocation. We evaluate PRIME using full-wave electromagnetic simulations, which enhance the accuracy of the extracted results. We also discuss the linear relationship between each user's pricing level and their received performance. The computational complexity and required computational time with different hardware

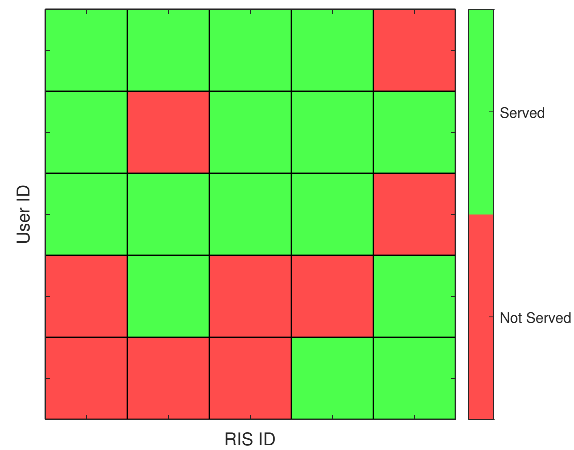

(a) Assignement of RIS to users

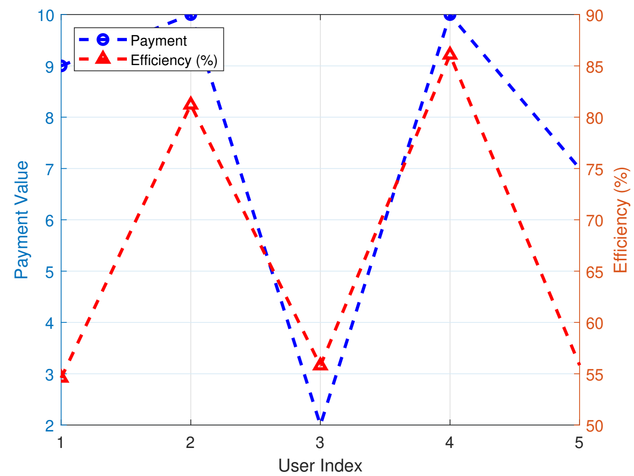

(b) Efficiency of each user.

Fig. 12: Cascaded link of 5 users with 5 RIS units.

setups indicate that PRIME can be effectively applied in real-world scenarios.

Acknowledgment

This work was funded by the German Federal Ministry of Education and Research (BMBF), grant 16KISK020K (6G-RIC), 2021-2025, the WISAR project for theoretical design and NATWORK project under Grant Agreement No. 101139285, for practical design.

References

[1] C. Liaskos, L. Mamatas, A. Pourdamghani, A. Tsioliaridou, S. Ioannidis, A. Pitsillides, S. Schmid, and I. F. Akyildiz, "Software-defined reconfigurable intelligent surfaces: From theory to end-to-end implementation," *Proceedings of the IEEE*, vol. 110, no. 9, pp. 1466–1493, 2022.

[2] C. Liaskos *et al.*, "Using any surface to realize a new paradigm for wireless communications," *Commun. ACM*, vol. 61, pp. 30–33, 2018.

[3] J. Bae, W. Khalid, A. Lee, H. Lee, S. Noh, and H. Yu, "Overview of ris-enabled secure transmission in 6g wireless networks," *Digital Communications and Networks*, 2024.

[4] H. Zhang, J. Hu, H. Zhang, B. Di, K. Bian, Z. Han, and L. Song, "Metaradar: Indoor localization by reconfigurable metamaterials," *IEEE Transactions on Mobile Computing*, vol. 21, no. 8, pp. 2895–2908, 2022.

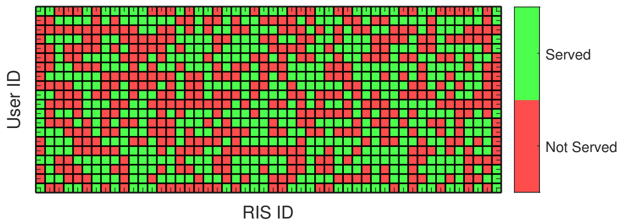

(a) Assignement of RIS to users

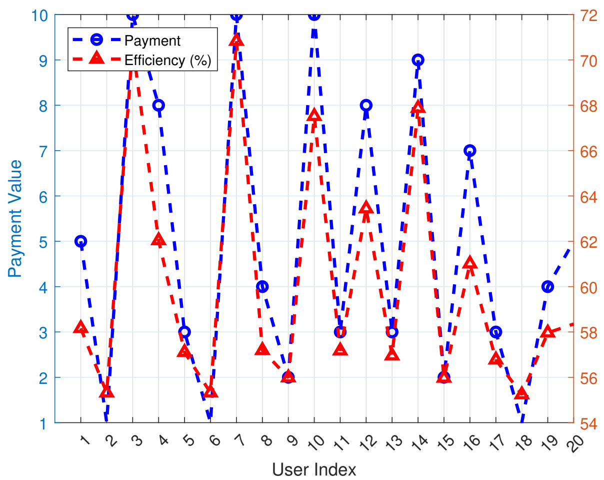

(b) Efficiency of each user.

Fig. 13: Cascaded link of 5 users with 5 RIS units.

[5] E. Basar, "Reconfigurable intelligent surfaces for doppler effect and multipath fading mitigation," *frontiers in Communications and Networks*, vol. 2, p. 672857, 2021.

[6] C. K. Liaskos, S. G. Petridou, and G. I. Papadimitriou, "Towards realizable, low-cost broadcast systems for dynamic environments," *IEEE/ACM Transactions on Networking*, vol. 19, no. 2, pp. 383–392, 2010.

[7] C. Liaskos, K. Katsalis, J. Triay, and S. Schmid, "Resource management for programmable metasurfaces: Concept, prospects and challenges," *IEEE Communications Magazine*, vol. 61, no. 11, pp. 208–214, 2023.

[8] C. Liaskos and K. Katsalis, "A scheduling framework for performing resource slicing with guarantees in 6g ris-enabled smart radio environments," *ITUJournal*, vol. 4, no. 1, pp. 33–49, 2023.

[9] S. I. Raptis *et al.*, "An accurate semi-analytical model for periodic tunable metasurfaces electromagnetic response," in *2024 18th European Conference on Antennas and Propagation (EuCAP)*, pp. 1–5, 2024.

[10] A. Pitilakis *et al.*, "Multifunctional metasurface architecture for amplitude, polarization and wave-front control," *Physical Review Applied*, vol. 17, no. 6, p. 064060, 2022.

[11] A. Lalas, N. Kantartzis, and T. Tsiboukis, "Programmable terahertz metamaterials through v-beam electrothermal devices," *Applied Physics A*, vol. 117, pp. 433–438, 2014.

[12] A. X. Lalas, N. V. Kantartzis, and T. D. Tsiboukis, "Reconfigurable metamaterial components exploiting two-hot-arm electrothermal actuators," *Microsystem Technologies*, vol. 21, pp. 2097–2107, 2015.

[13] A. Li *et al.*, "Metasurfaces and their applications," *Nanophotonics*, vol. 7, no. 6, pp. 989–1011, 2018.

[14] I. A. Papadopoulos *et al.*, "Physics-informed metaheuristics for fast ris codebook compilation," *IEEE Communications Magazine*, 2024.

[15] M. Segata, P. Casari, M. Lestas, A. Papadopoulos, D. Tyrovolas, T. Saeed, G. Karagiannidis, and C. Liaskos, "Cooperis: A framework for the simulation of reconfigurable intelligent surfaces in cooperative driving environments," *Computer Networks*, p. 110443, 2024.

[16] A. Papadopoulos *et al.*, "Ris as a network resource: User multiplexing and pricing algorithms," in *2024 3rd International Conference on 6G Networking (6GNet)*, pp. 144–152, 2024.

[17] M. Uchida and J. Kurose, "An information-theoretic characterization of weighted α-proportional fairness in network resource allocation," *Information Sciences*, vol. 181, no. 18, pp. 4009–4023, 2011.

[18] C. Avin, K. Mondal, and S. Schmid, "Demand-aware network design with minimal congestion and route lengths," *IEEE/ACM Transactions on Networking*, vol. 30, no. 4, pp. 1838–1848, 2022.

[19] J. Feng, Q. Pei, F. R. Yu, X. Chu, J. Du, and L. Zhu, "Dynamic network slicing and resource allocation in mobile edge computing systems," *IEEE Transactions on Vehicular Technology*, vol. 69, no. 7, pp. 7863–7878, 2020.

[20] Y. Abiko, T. Saito, D. Ikeda, K. Ohta, T. Mizuno, and H. Mineno, "Flexible resource block allocation to multiple slices for radio access network slicing using deep reinforcement learning," *IEEE Access*, vol. 8, pp. 68183–68198, 2020.

[21] F. Fossati, S. Moretti, P. Perny, and S. Secci, "Multi-resource allocation for network slicing," *IEEE/ACM Transactions on Networking*, vol. 28, no. 3, pp. 1311–1324, 2020.

[22] I. Chang, T. Ji, R. Zhu, Z. Wu, C. Li, and Y. Jiang, "Towards an efficient and dynamic allocation of radio access network slicing resources for 5g era," *IEEE Access*, 2023.

[23] O. Michel, R. Bifulco, G. Retvari, and S. Schmid, "The programmable data plane: Abstractions, architectures, algorithms, and applications," *ACM Computing Surveys (CSUR)*, vol. 54, no. 4, pp. 1–36, 2021.

[24] M. Leconte, G. S. Paschos, P. Mertikopoulos, and U. C. Kozat, "A resource allocation framework for network slicing," in *IEEE INFOCOM 2018-IEEE Conference on Computer Communications*, pp. 2177–2185, IEEE, 2018.

[25] M. Rost and S. Schmid, "Virtual network embedding approximations: Leveraging randomized rounding," *IEEE/ACM Transactions on Networking*, vol. 27, no. 5, pp. 2071–2084, 2019.

[26] Y. Zhang and H. Xu, "Optimal resource allocation for reconfigurable intelligent surface assisted dynamic wireless network via online reinforcement learning," in *2022 IEEE International Conference on Sensing, Communication, and Networking (SECON Workshops)*, pp. 13–18, IEEE, 2022.

[27] H. Zarini, N. Gholipoor, M. R. Mili, M. Rasti, H. Tabassum, and E. Hossain, "Resource management for multiplexing embb and urllc services over ris-aided thz communication," *IEEE Transactions on Communications*, vol. 71, no. 2, pp. 1207–1225, 2023.

[28] Z. Yang, M. Chen, W. Saad, W. Xu, M. Shikh-Bahaei, H. V. Poor, and S. Cui, "Resource allocation for wireless communications with distributed reconfigurable intelligent surfaces," in *GLOBECOM 2020-2020 IEEE Global Communications Conference*, pp. 1–6, IEEE, 2020.

[29] C. Battiloro, M. Merluzzi, P. Di Lorenzo, and S. Barbarossa, "Dynamic resource optimization for adaptive federated learning empowered by reconfigurable intelligent surfaces," in *ICASSP 2022-2022 IEEE International Conference on Acoustics, Speech and Signal Processing (ICASSP)*, pp. 4083–4087, IEEE, 2022.

[30] S. Lin, Y. Zou, J. Zhu, H. Guo, B. Li, and F. Xie, "Outage probability analysis of ris-assisted wireless powered multi-user communications," in *2021 13th International Conference on Wireless Communications and Signal Processing (WCSP)*, pp. 1–5, 2021.

[31] The VISORSURF consortium, *The Internet of Materials*. CRC Press, 2020.

[32] M. Stănculescu *et al.*, "Using s parameters in wireless power transfer analysis," in *2017 10th International Symposium on Advanced Topics in Electrical Engineering (ATEE)*, pp. 107–112, IEEE, 2017.

[33] A. Papadopoulos *et al.*, "An open platform for simulating the physical layer of 6g communication systems with multiple intelligent surfaces," in *2022 18th International Conference on Network and Service Management (CNSM)*, pp. 359–363, IEEE, 2022.

[34] S. Luke, *Essentials of Metaheuristics*. Lulu, second ed., 2013. Available for free at http://cs.gmu.edu/∼sean/book/metaheuristics/.